RSC Advances

ROYAL SOCIETY OF CHEMISTRY

www.rsc.org/advances

A table of contents entry

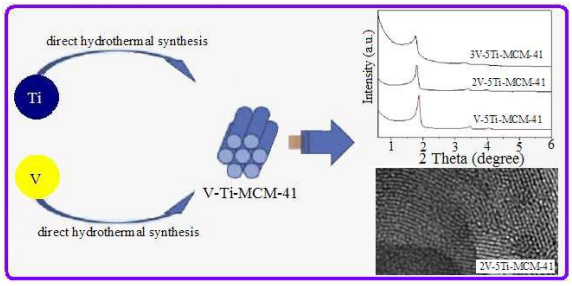

V and Ti atoms incorporated into the framework of MCM-41 in the form of tetrahedral coordination with excellent catalytic performance.

RSC Advances

RSCPublishing

ARTICLE

Bimetallic V and Ti incorporated MCM-41 molecular sieves and its catalytic properties

Cite this: DOI: 10.1039/x0xx00000x

Baoshan Li*, Naijin Wu, Kai Wu, Jianjun Liu, Chunying Han, Xianfen Li

Received 00th January 2012,
Accepted 00th January 2012

DOI: 10.1039/x0xx00000x

www.rsc.org/

A series of bimetallic mesostructured V-Ti-MCM-41 molecular sieves with high surface area and narrow pore-size distribution were obtained by hydrothermal crystallization method. The obtained products were characterized by a series of techniques including X-ray fluorescence, X-ray diffraction, high-resolution transmission electron microscopy, N_2 adsorption-desorption, Fourier-transform infrared spectroscopy, X-ray photoelectron spectroscopy and diffuse reflectance ultraviolet–visible spectroscopy. Characterization results showed that the V-Ti-MCM-41 samples remain a relative ordered hexagonal structure. V and Ti atoms were incorporated into the silicon framework. The highest phenol selectivity of 94.7% and benzene conversion of 22.3% are obtained over 3V-5Ti-MCM-41 sample using H_2O_2 as oxidant. In addition, the catalytic performance did not decrease after being recycled four times.

1. Introduction

MCM-41 molecular sieves, with high surface areas, regularly ordered pore arrangements, narrow and adjustable pore size distributions in the range of 2-10 nm or larger, and relatively high thermal stabilities, could be widely used in catalysis, sorption and separation[1-4]. However, pure M41S materials showed very limited catalytic activity which attribute to their low hydrothermal stability and poor acidity[5-8]. Hence a large series of single metal ions such as Fe [9], V[10], Ti[11], Ni[12], Co[13], Cu[14], Pt[15] have been used to modify the MCM-41 silica framework to increase the active sites and improve the catalytic activity. Some of these materials have shown high catalytic activities in the selective oxidation, hydroxylation, oxidative desulfurization, adsorptive desulfurization and hydrocracking of organic compounds but low selectivity[16-19], and others have shown the inverse results[20, 21]. Most of the reports in the literature were focused on mesoporous molecular sieves incorporated with mono-kind of metal in last decades, only a few studies concerned the synthesis and catalysis of bimetallic ions modified mesoporous molecular sieves, mostly due to the hard control of the simultaneous hydrolyzation of multi-kind of metal and silicon species[22,23]. Multi-component incorporation can modify the surface properties of mesoporous silicate which is more effective than mono-kind of heteroatom incorporation[24,25]. Therefore, the incorporation of two different metals might create new materials with new redox and acid properties. J. J. Zou et al. reported the synthesis and catalytic property of M-Ti-MCM41 (M= V, Fe Cr)[26-28]. It has been found that the acidity increased as metal was incorporated into Ti-MCM-41 and the metal-incorporated materials show improved photocatalytic activity under UV irradiation, with the role order of V- > Fe- > Cr-incorporation. V. Parvulescu et al. designed a bimetallic Co-M-modified MCM-41 catalysts (M= V, Nb, La) for oxidation of styrene and benzene with hydrogen peroxide[29]. The results revealed that the Co-Nb catalysts exhibited high conversion of the styrene and the Co-V catalysts exhibited high conversion of benzene. V. Parvulescu and his group also prepared bimetallic Ru-(Cr, Ni, or Cu) and La-(Co or Mn) incorporated MCM-41 for oxidation of aromatic hydrocarbons[30]. They found the obtained samples showed high activity and selectivity in oxidation of styrene and benzene with hydrogen peroxide. X. Z. Duan et al. reported hydrogen production by ammonia decomposition with Co-Mo/MCM-41 catalyst[31]. The highest conversion of NH_3 was up to 99.2%.

Phenol is an important intermediate used in the synthesis of phenol resins, bisphenol-A, caprolactam, etc. Industrially, phenol is produced mainly through the three-step cumene process, which suffers from a low one-pass yield of phenol, a low atomic efficiency and an equimolar amount of acetone byproduct. Several studies have been published during the past two decades on the synthesis of phenol via one-step oxidation of benzene. Direct hydroxylation of the aromatic ring is a challenging reaction to synthesize phenol, due to the formation of over-oxygenated by-products. The synthesis of phenol by direct hydroxylation of benzene was extensively studied using different oxidants, such as O_2[32], H_2O_2[33] and N_2O[34]. Y. Kong et al. studied the hydroxylation of benzene reaction over Cu-MCM-41 with H_2O_2 as oxidant[35], Cu-MCM-41 showed excellent catalytic activity in the direct hydroxylation of benzene. J. He et al. found that the highest phenol selectivity was 94% using Fe-MCM-41 as catalysts with H_2O_2[36]. C. W. Lee reported hydroxylation of benzene with vanadium-containing molecular sieves catalyst using H_2O_2 as

oxidant[37]. The selectivity of phenol was very high and the catalysts are stable. K. Wu et al.[10] reported the catalytic performance of V-MCM-41 for the selective oxidation of cyclohexane for producing KA oil. They found that the conversion of cyclohexane and the selectivity of KA oil increased with the vanadium content increase in the frameworks, and the conversion and selectivity were higher than that over the loaded V/MCM-41 catalysts with the same V content. So it is meaningful to increase the V content in the framework of MCM-41.

In this paper, V-Ti-MCM-41 with different vanadium and titanium contents were synthesized and the highest vanadium and titanium content was 3.5 wt% and 6.1 wt%, respectivity. The resulting samples were characterized by a series of physicochemical techniques, the results revealed that the vanadium and titanium atoms were highly dispersed and incorporated into the framework of MCM-41.

2. Experimental section

2.1 Preparation of V-Ti-MCM-41

V-Ti-MCM-41 with different vanadium and titanium content was synthesized as follows: 4.0 g of cetyltrimethylammonium bromide (CTAB) was dissolved in 60 ml of deionized water and stirred until a clear solution was obtained. Amount of calculation of ammonium vanadate, oxalic acid and deionized water were mixed and heated at 100 ◦C until a blue clear solution was obtained. Then 10 ml of tartaric acid was added into the blue solution to obtain a complexing solution. Amount of calculation of titanium (IV) tetrabutoxide (TBOT), 20 ml ethanol and the complexing solution was added into the above CTAB solution. After stirring for 1 h, amount of calculation tetraethyl orthosilicate (TEOS) was added dropwise to the solution and stirring for 6 h. The pH was adjusted to 9.5 using ammonia. The resulting gel was transferred into a Teflon-lined autoclave and heated at 373 K under autogenously pressure for 72 h. The product was collected by filtration, washed with deionized water, dried at 110 ◦C and then calcined in air at 550 ◦C for 6 h to remove the template.

2.2 Characterizations

The vanadium and titanium content of the samples was measured by using X-ray fluorescence (XRF) analysis on a Philips Magix-601 X-ray fluorescence spectrometer. The X-ray diffraction (XRD) patterns were recorded on a Rigaku D/Max 2500 VBZ+/PC diffractometer using Cu-Kα radiation (λ= 0.1541 nm) over the 2θ range of low-angle 0.5-6^o and wide-angle range 10-70^o, respectively. The pore morphology of the sample was examined by high-resolution transmission electron microscopy (HRTEM) on a Jem-3010 with an accelerating voltage of 200 kV. The nitrogen adsorption-desorption isotherm of the sample was carried out by using a Quantachrome Autosorb-1 volumetric adsorption analyzer. The specific surface area (S_{BET}) was estimated by BET method and the pore size distribution was calculated through BJH method. Before the nitrogen adsorption, the sample was pretreated for degassing in vacuum at 200 ^{o}C for 5 h. The Fourier transform infrared (FT-IR) spectra over the range of 4000-400 cm^{-1} were recorded on a Thermo Nicolet Nexus 470 spectrometer using a KBr disc. The X-ray photoelectron spectroscopy (XPS) analysis was conducted on an ESCALAB 250 spectrometer equipped with an Al-Kα X-ray source. The carbon 1s peak at 284.6 eV was used as the reference for binding energies. The diffuse reflectance ultraviolet–visible spectroscopy (DRUV–vis) was obtained on a Hitachi Model U-3010 spectrophotometer over the wavelength 200–500 nm using $BaSO_4$ as the reference.

2.3 Catalytic performance test

The hydroxylation of benzene was carried out in a three-necked flask. In a typical run, 5 ml benzene and 0.5 g catalyst was added into the flask. Then, 3 ml 30% H_2O_2 was added into the flask and stirred for 5 h at 30 ^{o}C. At end of the reaction, the solid catalyst was filtrated and washed with benzene and dried at room temperature. and the organic products were analyzed by a HP5890 series gas chromatography equipped with a SPB-50 coated capillary column (30 m × 0.32 mm × 0.25 μm) and FID. The main products of the reaction were phenol, which were confirmed by GC-MS.

3. Results and discussion

3.1 Characterization

The XRF analysis results were listed in **Table 1**. The content of vanadium is 1.2wt.%, 2.3wt.% and 3.5wt.% and the content of titanium is 6.1wt.% in the three samples. The molar ratio of vanadium and titanium is 1:5, 2:5 and 3:5, which was named as V-5Ti-MCM-41, 2V-5Ti-MCM-41, and 3V-5Ti-MCM-41, respectively.

Table 1. Structure properties of the V-Ti-MCM-41 samples.

Sample	V (wt.%)	Ti (wt.%)	Molar ratio (V/Ti)	S_{BET} (m^2 g^{-1})	V_p (cm^3 g^{-1})	R_p (nm)
V-5Ti-MCM-41	1.2	6.1	1:5	721	0.72	2.7
2V-5Ti-MCM-41	2.3	6.1	2:5	684	0.61	3.0
3V-5Ti-MCM-41	3.5	6.1	3:5	621	0.54	3.3

The small-angle XRD patterns of the samples are presented in **Fig. 1A**. All the samples showed one major, assigned to reflection line of (1 0 0), and two weak peaks, corresponding to reflection lines of (1 1 0) and (2 0 0). The (1 0 0) peak is shifted to the smaller angle with the molar ratio of vanadium and titanium increasing. All the samples have good ordered hexagonal mesostructure of MCM-41 and the shifting can be attributed to the incorporation of vanadium and titanium atoms into the mesostructure.

The wide-angle XRD patterns of the V-Ti-MCM-41 samples are shown in **Fig. 1B**. No peak appearance corresponding to the crystalline vanadium oxides in all the three samples, which suggested that vanadium species might be in the framework or highly dispersed on the surface of the V-Ti-MCM-41.

The HRTEM images (**Fig. 2**) of the bimetallic mesoporous molecular sieves are characteristics for the mesoporous materials with hexagonal channel array, showing high quality in organization of channels of these samples. The HRTEM images confirm the well-

organized hexagonal pore system for these samples and a slight degradation of the structure for 3V-5Ti-MCM-41 samples. The results are in consistent with the XRD analysis. Vanadium and titanium atoms were enchased uniformly in the framework or highly dispersed in the matrix of the MCM-41 and no VO*x* and TiO*x* particles appear on V-Ti-MCM-41 samples.

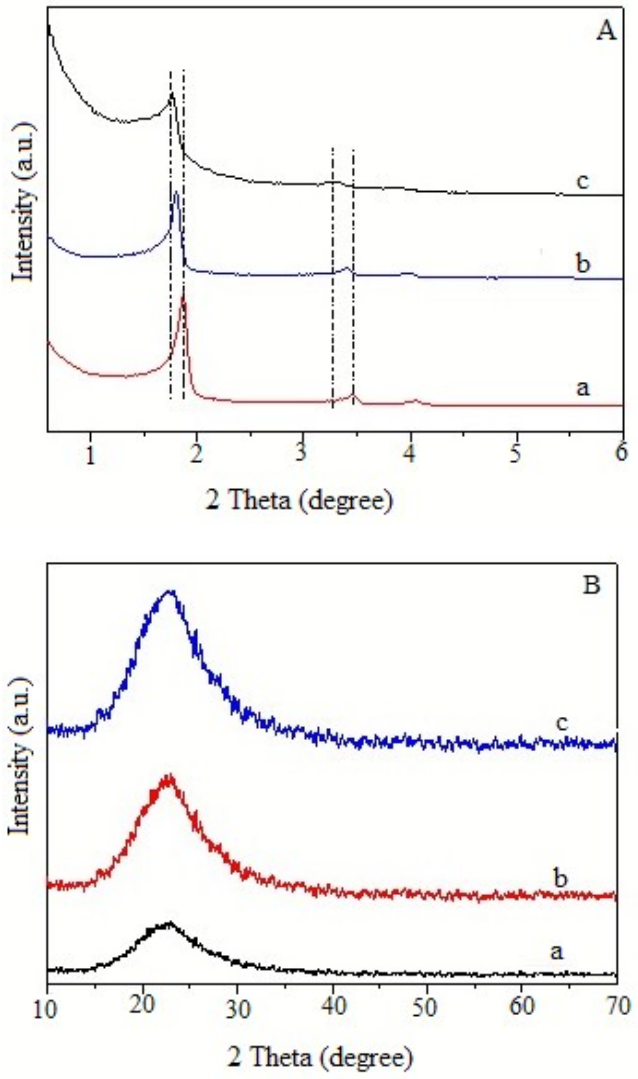

Figure 1. Small-angle XRD patterns (A) and wide-angle XRD patterns (B) of the V-Ti-MCM-41 samples: (a) V-5Ti-MCM-41, (b) 2V-5Ti-MCM-41, and (c) 3V-5Ti-MCM-41.

The N_2 adsorption-desorption isotherms of the V-Ti-MCM-41 samples are shown in Fig. 3A. The results showed that V-Ti-MCM-41 exhibits a typical type IV isotherm[38], indicating a highly ordered mesoporous structure. Well-defined mesoporosity results in a high surface area 621 m^2 g^{-1} and narrow pore size distribution with a mean diameter of 3.3 nm, as shown in Table 1. The pore size distribution curves of V-Ti-MCM-41 samples are presented in Fig. 3B and the pore structure parameters are listed in Table 1. The surface areas and pore volumes of the samples decrease with the increase of molar ratio of vanadium and titanium, which are ascribed to the vanadium and titanium entering the framework of MCM-41. Because the diameter of vanadium and titanium atom is much larger than that of silicon atom, as the small silicon atom was substituted

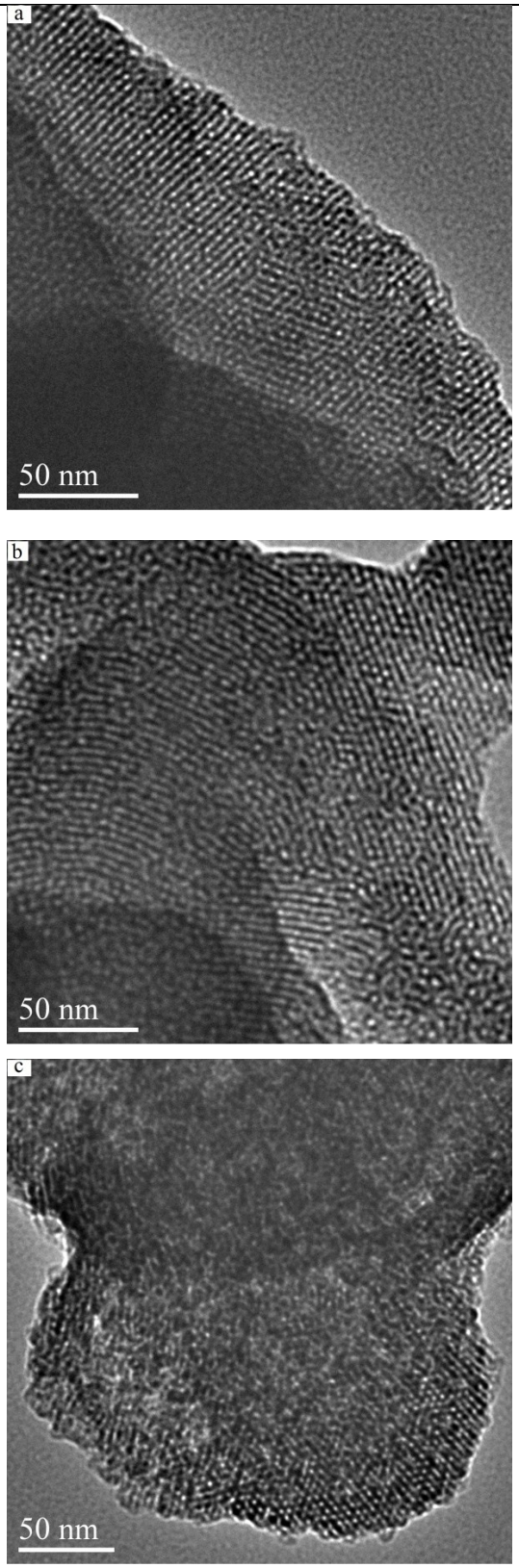

Figure 2. The HRTEM images of the V-Ti-MCM-41 samples: (a) V-5Ti-MCM-41, (b) 2V-5Ti-MCM-41, and (c) 3V-5Ti-MCM-41.

by the large vanadium and titanium atom in the framework the pore radius (R_p) was enlarged, the more silicon atoms were substituted the

larger of the R_p. On the other hand, the weights of vanadium and titanium atom are much larger than that of siliconatom, which is the main reason that induced the decreasing of specific surface area (S_{BET}) and pore volume (V_p).

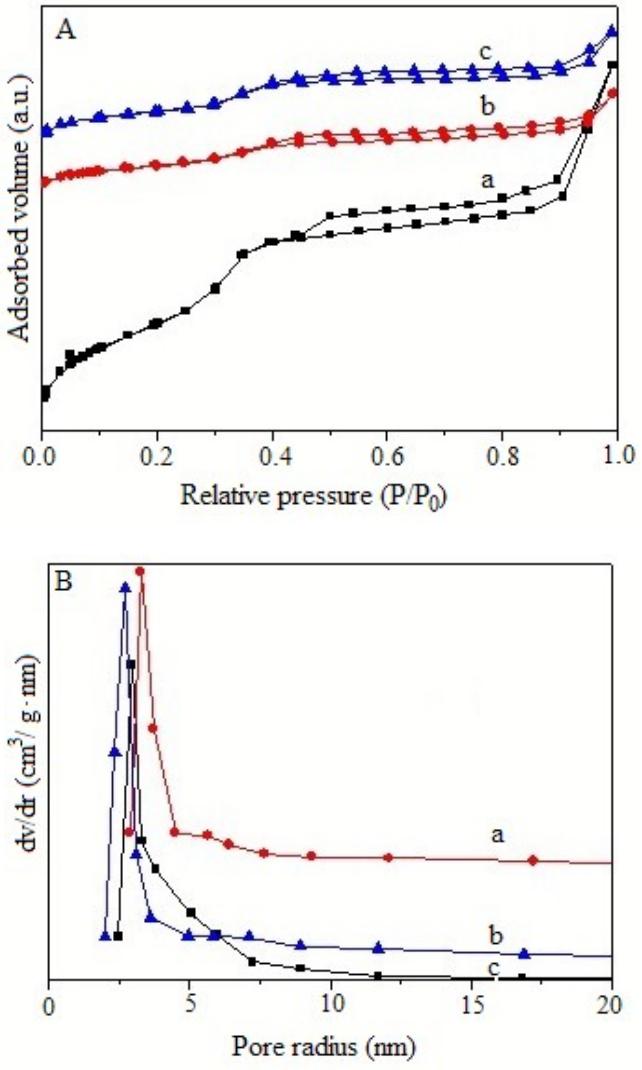

Figure 3. N_2 adsorption-desorption isotherms (A) and pore size distribution curves (B) of the V-Ti-MCM-41 samples: (a) 3V-5Ti-MCM-41, (b) 2V-5Ti-MCM-41, and (c) V-5Ti-MCM-41.

The FT-IR absorbance spectra of the V-Ti-MCM-41 samples are depicted in **Fig. 4**. All the samples exhibit a symmetric stretching vibration band at around 806 cm^{-1} and the asymmetric vibration band at around 1098 cm^{-1} of the tetrahedral SiO_4^{4-} structural units. The band at around 463 cm^{-1} can be assigned to bending modes of Si-O-Si bond. As the heteroatoms were introduced to MCM-41, a slight red shift was observed for 1098 and 806 cm^{-1}. It was suggested that there was a strong interaction between the atoms of vanadium, titanium and silicon, and the presence of red shift appears to be the possible evidence of the isomorphous substitution of Si by metal ions. The heteroatoms were incorporated into the framework of MCM-41 and M-O-Si bonds were formed. The ion radii of vanadium (IV) and titanium (IV) were all larger than silicon (IV), and the length of M-O (M = V and Ti) was greater than that of Si-O, which led to the decrease of the force constant (k) of the bands. The atomic weights of vanadium and titanium were all bigger than that of silicon, thus the reduced mass (μ) would increase, hence the vibration frequencies (ν) calculated from the formula $\nu = \frac{1}{2\pi}\sqrt{\frac{k}{\mu}}$ decreased [39].

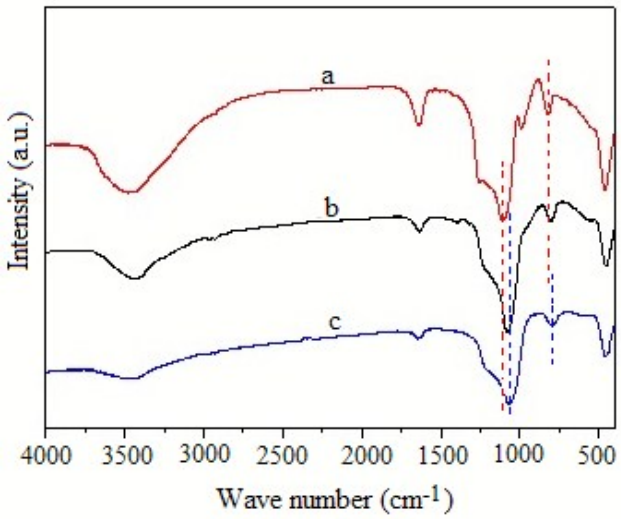

Figure 4. FT-IR spectra of the V-Ti-MCM-41 samples: (a) V-5Ti-MCM-41, (b) 2V-5Ti-MCM-41, and (c) 3V-5Ti-MCM-41

The XPS spectrum of 3V-5Ti-MCM-41 is depicted in **Fig. 5** (the complete XPS spectrum of V in 3V-5Ti-MCM-41 is depicted in Fig. S1†). The peaks at the binding energy of 516 (**Fig. 5A**) and 459.7 eV (**Fig. 5B**) are ascribed to V2p3/2 of the V^{4+} and Ti2p3/2 of the Ti^{4+}, respectively[11, 40]. Moreover, no peaks appear at the binding energy of 517 and 458.5 eV corresponding to V^{5+} and octahedral coordination of Ti^{4+}, which suggests the vanadium and titanium species are exclusively in the tetrahedral coordination in the framework[11, 41].

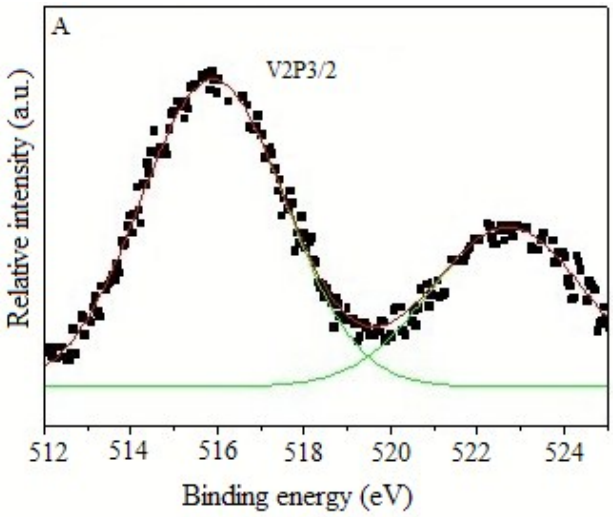

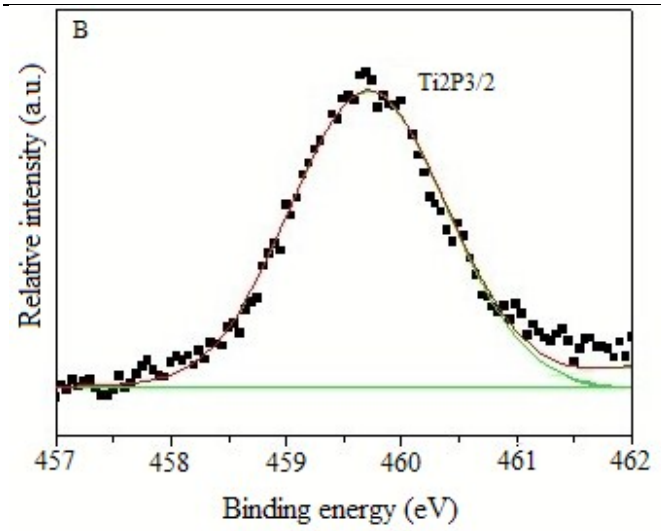

Figure 5. The XPS spectrum of V (A) and Ti (B) in 3V-5Ti-MCM-41.

Figure 6 shows the UV-vis spectra of the synthesized samples. The absorption in the region of < 230 nm can be ascribed to the charge transfer from the lattice oxygen (O^{2-}) to Ti species in tetrahedral coordination, which has been widely found for Ti-substituted zeolites and is characteristic of tetrahedrally coordinated Ti highly dispersed in the framework. The absorption centered around 260 nm can be ascribed to the charge transfer from the lattice oxygen (O^{2-}) to V^{4+} in tetrahedral coordination[42,43]. And there is no any absorption in the region of >330 nm. It has been reported that the band around 258 nm is associated to V and Ti species in 4-fold coordination state[28]. One can conclude that V and Ti ions are highly dispersed in MCM-41 framework at atomic level with tetrahedral coordination.

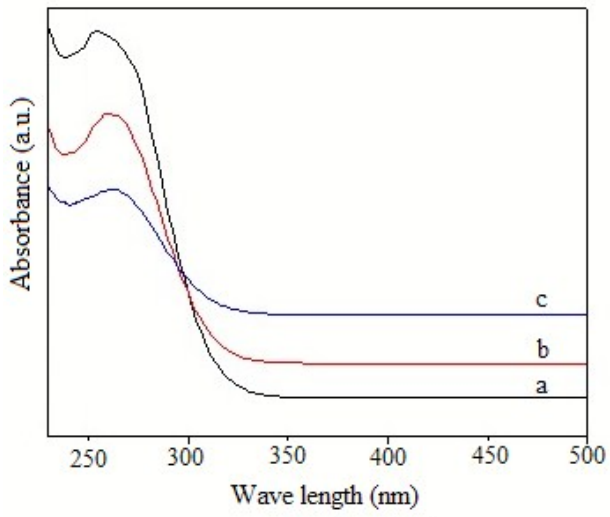

Figure 6. UV-vis spectra of the samples: (a) V-5Ti-MCM-41, (b) 2V-5Ti-MCM-41, and (c) 3V-5Ti-MCM-41

3.2 Catalytic performance

Phenol was the main products in the hydroxylation of benzene with H_2O_2 as oxidation over V-Ti-MCM-41 catalyst and the results are shown in **Table 2**. It is obviously that the V-Ti-MCM-41 samples exhibit an outstanding conversion and high selectivity toward phenol, which are due to the fact that the incorporation of vanadium and titanium into the MCM-41, indicating that the vanadium and titanium atoms are the active component for the reaction. The conversion of benzene increased with the vanadium content increase, and the conversion was up to 22.3% over the 3V-5Ti-MCM-41 catalyst, which illuminates that the catalytic properties are sensitive to the content of vanadium and titanium introduced. Moreover, the selectivity of phenol increased gradually with increasing vanadium incorporation and the highest selectivity of phenol was 94.7% over the 3V-5Ti-MCM-41.

Table 2. Catalytic performance of the samples

Sample	Recycling times	Conversion (%)	Selectivity (%)	
			Phenol	Others
V-5Ti-MCM-41	1	15.1	88.2	11.8
2V-5Ti-MCM-41	1	18.5	91.4	8.6
3V-5Ti-MCM-41	1	22.3	94.7	5.3
	2	22.3	94.6	5.4
	3	22.4	94.3	5.3
	4	22.3	94.5	5.5

The catalyst recycling test was also conducted and the results are shown in **Table 2**. It is obvious that the sample 3V-5Ti-MCM-41 could be reused for four times and its catalytic activity and selectivity did not decrease, indicating the 3V-5Ti-MCM-41 sample was stable.

4. Conclusion

A series of V-Ti-MCM-41 samples with different vanadium and titanium contents have been synthesized by the simple hydrothermal crystallization method. The samples reveal a regular hexagonal array of uniform channels and all vanadium and titanium atoms are incorporated into the framework of MCM-41. The catalytic performance was excellent for the hydroxylation of benzene and the sample 3V-5Ti-MCM-41 showed good stability.

Acknowledgment

The work was supported by the National Natural Science of Foundation of China (No. 21271017) and the Fundamental Research Funds for the Central Universities (YS1406). The X-ray absorption experiments at the Fe K edge were performed at the U7C beamline of National Synchrotron Radiation Laboratory (NSRL), China.

Notes and references

State Key Laboratory of Chemical Resource Engineering, Beijing University of Chemical Technology, No. 15 Beisanhuan East Road, Beijing 100029, P. R. China. Fax: (+) 86-010-64445611; Tel: (+) 86-010-64445611; E-mail: bsli@mail.buct.edu.cn

1 B. Q. Han, F. Zhang, Z. P. Feng, S. Y. Liu, S. J. Deng, Y. Wang, Y. D. Wang. *Ceram. Int.*, 2014, **40** , 8093.

2 Y. F. Shao, B. Yan. *Micropor. Mesopor. Mater.,* 2014, **193**, 85.

3 J. F. Lin, B. H. Zhao, Y. Cao, H. Xu, S. H. Ma, M. Y. Guo, D. R. Qiao, Y. Cao. *Appl. Catal. A: Gen*., 2014, **478**, 175.

4 P. Carraro, V. Elías, A. A. G. Blanco, K. Sapag, G. Eimer, M. Oliva. Int. *J. Hydrogen Energy*.,2014, **39**, 8749.

5 Z. Gholami, A. Z. Abdullah, K. T. Lee. *Appl. Catal. A: Gen*., 2014, **479**, 76.

6 J. Zang, Y. J. Ding, L. Yan, T. Wang, Y. Lu, L. F. Gong. *Catal. Commun.*, 2014, **51**, 24.

7 A. M. Akondi, M. L. Kantam, R. Trivedi, B. Sreedhar, S. K. Buddana, R. S. Prakasham, S. Bhargava. J. Mol. Catal. A: Chem. 386 (2014) 49-60.

8 A. Patel, S. Singh. *Micropor. Mesopor. Mater*., 2014, **195**, 240.

9 B. S. Li, K. Wu, T. H. Yuan, C. Y. Han, J. Q. Xu, X. M. Pang. *Micropor. Mesopor. Mater.*, 2012, **151**, 277.

10 K. Wu, B. S. Li, C. Y. Han, J. J. Liu. *Appl. Catal. A: Gen.*, 2014, **479**, 70.

11 S. P. Wang, Y. Shi, X. B. Ma. *Micropor. Mesopor. Mater*., 2012, **156**, 22.

12 N. J. Wu, W. Zhang, B. S. Li, C. Y. Han. *Micropor. Mesopor. Mater.*, 2014, **185**, 130.

13 B. Han, H. Q. Wang, Y. Kong, J. Wang. *Mater. Lett*., 2013, **100**, 159.

14 J. Qiu, K. Zhuang, M. Lu, B. L. Xu, Y. N. Fan. *Catal. Commun*., 2013, **31**, 21.

15 H. P. Liu, G. Z. Lu, Y. Guo, Y. Q. Wang, Y. L. Guo. *J. Colloid Interface Sci*., 2010, **346**, 486.

16 M. Karthik, H. Bai. *Appl. Catal. B: Environ*., 2014, **144**, 809.

17 M. Chatterjee, T. Ishizaka, H. Kawanami. *J. Colloid Interface Sci*., 2014, **420**, 15.

18 B. Qi, L. L. Lou, Y. B. Wang, K. Yu, Y. Yang, S. X. Liu. *Micropor. Mesopor. Mater*., 2014, **190**, 275.

19 D. W. He, C. C. Bai, C. W. Jiang, T. Zhou. *Powder Technol.*, 2013, **249**, 151.

20 L. Ma, J. B. Ji, F. W. Yu, N. Ai, H. T. Jiang. *Micropor. Mesopor. Mater.*, 2013, **165**, 6.

21 K. N. Tayade, M. Mishra. *J. Mol. Catal. A: Chem*., 2014, **382**, 114.

22 D. P. Liu, X. Y. Quek, W. N. E. Cheo, R. Lau, A. Borgna, Y. H. Yang. *J. Catal*., 2009, **266**, 380.

23 R. Atchudan, A. Pandurangan. J. Mol. Catal. A: Chem. 355 (2012) 75-84.

24 K. Rintramee, K. Föttinger, G. Rupprechter, J. Wittayakun. *Appl. Catal. B: Environ.*, 2012, **115-116**, 225.

25 C. Z. Loebick, S. Lee, S. Derrouiche, M. Schwab, Y. Chen, G. L. Haller, L. Pfefferle. *J. Catal*., 2010, **271**, 358.

26 J. J. Zou, Y. Liu, L. Pan, L. Wang, X. W. Zhang. *Appl. Catal. B: Environ.*, 2010, **95**, 439.

27 V.-H. Nguyen, H.-Y. Chan, J. C.S. Wu, H. Bai. *Chem. Eng. J.*, 2012,**179**,285.

28 J.-J. Zou, Y. Liu, L. Pan, L. Wang, X. Zhang. *Appl. Catal. B: Environ.*, 2010, **l 95** ,439.

29 V. Parvulescu, C. Tablet, C. Anastasescu, B. L. Su. *Catal. Today*., 2004, **93-95**, 307.

30 V. Parvulescu, C. Anastasescu, B. L. Su. *J. Mol. Catal. A: Chem*., 2004, **211**, 143.

31 X. Z. Duan, G. Qian, X. G. Zhou, D. Chen, W. K. Yuan. *Chem. Eng. J.*, 2012, **207-208**, 103.

32 Z. Y. Long, Y. Zhou, G. J. Chen, P. P. Zhao, J. Wang. *Chem. Eng. J*., 2014, **239**, 19.

33 L. Y. Hu, B. Yue, C. Wang, X. Y. Chen, H. Y. He. *Appl. Catal. A: Gen*., 2014, **477**, 141.

34 G. Centi, S. Perathoner, F. Pino, R. Arrigo, G. Giordano, A. Katovic, V. Pedulà. *Catal. Today.,* 2005, 110, 211.

35 Y. Kong, X. J. Xu, Y. Wu, R. Zhang, J. Wang. Chin. J. Catal. 29 (2008) 385-390.

36 J. He, Z. Y. Guo, H. Ma, D. G. Evans, X. Duan. Chin. *J. Catal*., 2002, **212**, 22.

37 C. W. Lee, W. J. Lee, Y. K. Park, S. E. Park. *Catal. Today*. 2000, **61**, 137.

38 V. Parvulescu, C. Anastasescu, C. Constantin, B. L. Su. *Catal. Today*, 2003, **78**, 477.

39 Y. Kong, S. Y. Jiang, J. Wang, S. S. Wang, Q. J. Yan, Y. N. Lu. *Micropor. Mesopor. Mater*., 2005, **86**, 191.

40 K. M. Lin, C. Lin, C. Hsiao, Y. Y. Li, *J. Lumin.,* 2007, 127, 561.

41 R. K. Jha, S. Shylesh, S. S. Bhoware, A. P. Singh, *Micropor. Mesopor. Mater.,* 2006, **95**, 154.

42 Y.-J. Do, J.-H. Kin, J.-H. Park, S.-S. Park, S.-S. Hong, C.-S. Suh, G.-D. Lee*, Catal. Today*,2005, **101**, 299.

43 X. Wang, W. Lian, X. Fu, J.-M. Basset, F. Lefebure*, J. Catal.* , 2006, **238,**13.